[Review Paper]

Carbon-supported PtSn Catalysts: Characterization and Catalytic Properties

Maria Carmen ROMÁN-MARTÍNEZ[†1)]*, Dego CAZORLA-AMORÓS[†1)], Sergio de MIGUEL[†2)], and Osvaldo SCELZA[†2)]

[†1)] Departamento de Química Inorgánica, Facultad de Ciencias, Universidad de Alicante, Apartado 99, 03080 Alicante, SPAIN
[†2)] Instituto de Investigaciones en Catálisis y Petroquímica (INCAPE), Facultad de Ingeniería Química, Universidad Nacional del Litoral, CONICET, Santiago del Estero 2654 (3000) Santa Fe, ARGENTINA

(Received November 4, 2003)

Carbon-supported PtSn catalysts were prepared by impregnation using a commercial activated carbon after purification and oxidation (H_2O_2, 20 v/v%) treatments. The support surface chemistry of the carbon after purification and the oxidized carbon, and successive impregnation or coimpregnation procedures were the variables investigated. The catalysts obtained were characterized using the following techniques: TPD and TPR experiments, H_2 chemisorption, XPS and XAFS, and activity assessment in the following reactions: cyclohexane dehydrogenation (reaction insensitive to structure), cyclopentane hydrogenolysis (reaction sensitive to structure) and carvone hydrogenation, which allows analysis of the selectivity of PtSn catalysts (carvone contains one C=O group and two C=C bonds for hydrogenation). The objective of the study is to find any relationships between the preparation procedure and the support properties, the characteristics of the resulting catalysts, and the catalytic behavior. The porosity of the carbon support together with the surface oxidation determines the accessibility of reactants to the active sites. Unusual selectivity to alcohols was found. Addition of tin caused blocking and dilution of the platinum clusters. The carbon support also affected the selectivity either because of its electronic properties or because of the particular metal structures developed.

Keywords
Platinum tin catalyst, Carbon support, Carvone hydrogenation, XAFS, TPR

1. Introduction

Supported bimetallic PtSn catalysts are widely used for reforming reactions in the petroleum industry and for selective hydrogenation reactions in fine chemistry[1)～3)]. Platinum modification by tin has different effects depending on the support, mainly because tin can not only modify the surface acidity, but also affects the metallic structures created after reduction, which are also determined by the nature and the pre-treatment of the support. Other important variables are the Pt/Sn ratio and the preparation procedures. The most outstanding property related to the addition of tin to platinum is the important modification of the selectivity, which in naphtha reforming reactions results in a higher stability against deactivation by coke deposition[3)].

Most investigations of PtSn catalysts have shown that the effects of tin on platinum are of both geometrical and electronic character, the former related with dilution (decrease of the cluster size) or blockage effects, and the latter involving the formation of PtSn alloys. In addition, the presence of ionic tin species is an important factor in the selectivity of reactions such as the hydrogenation of α,β-unsaturated aldehydes[4)].

Many investigations have attempted to obtain PtSn supported catalysts with both high selectivity and high catalytic activity. The basis must be to find out how can tin modify the catalytic properties of platinum and the tin species responsible of such a modification. Therefore, thorough characterization of the catalytic system is necessary to find the relationships between the preparation variables (including type of support and Pt/Sn ratio), the geometrical and electronic effect of tin on platinum, and the catalytic behavior. Many researchers have based their studies on this idea[5)～14)], but, unfortunately, no definite conclusions have been reached.

Characterization of supported Pt and Sn is frequently carried out by XPS (X-ray photoelectron spectroscopy)[8),10),13)～16)], XRD (X-ray diffraction)[8)], and H_2 or CO chemisorption measurements[10),13)]. Some studies also made use of techniques like Mösbauer spectroscopy[17),18)], TEM (transmission electron microscope)[8),13)], FTIR (fourier transform infrared spectroscopy)[15)], TPR (temperature programmed reduction)[10),19)], and XAFS

* To whom correspondence should be addressed.
* E-mail: mcroman@ua.es

(X-ray absorption fine structure)[11),16),20),21)]. XAFS is, nowadays, one of the most powerful methods for local-order characterization in highly dispersed metal catalysts[22)~25)].

The catalytic activity measurements usually deal with real reforming reactions or with fine chemistry syntheses. These reactions may provide interesting tests to infer the presence of specific catalytic structures.

Fine chemistry reactions include the hydrogenation of α,β-unsaturated aldehydes or ketones, as reviewed by Ponec[4)]. In this case, it is interesting to mention that the differences in the bonding of the C=C and C=O groups to the surface of the catalyst are the main factor determining the selectivity. The geometry and character of bonding of these two functionalities to the metal surfaces seem to be well established, but how many metal atoms combine to constitute an adsorption site is not known. In PtSn catalysts, Sn^{n+} is the effective promoter site for the hydrogenation of α,β-unsaturated aldehydes, whereas such promotion is not observed in the case of ketones[4)]. Recently, Sn^{n+} was suggested to be the species responsible for the selective formation of alcohol in the hydrogenation of crotonaldehyde over PdSn supported on silica and alumina[26)]. However, the selectivity effect of Sn in the hydrogenation of cinnamaldehyde over $PdSn/SiO_2$ is suggested mainly to be due to strong suppression of the adsorption/hydrogenation of the C=C double bond, rather than enhancement of the hydrogenation of the carbonyl group[27)].

The present paper reviews our recent results obtained in the investigation of PtSn catalysts supported on carbon[10),11),19)]. We would like to note that, in spite of the interesting properties of carbon as catalyst support[28),29)], research on PtSn catalysts supported on carbon materials is relatively scarce. Less than one tenth of papers deal with carbon-supported bimetallic catalysts, as most research uses Al_2O_3 and SiO_2 as supports. Our study of carbon-supported PtSn catalysts is based on our experience with Pt/carbon catalysts[30)~35)], as well as PtSn supported on inorganic oxides[15),19),36)~38)].

The catalysts were prepared using two activated carbons with different surface chemistry and two different sequences of impregnation: successive impregnation and coimpregnation. Several techniques were used to characterize the catalysts: TPD and TPR experiments, H_2 chemisorption, XPS (X-ray photoelectron spectra) and XAFS. The catalytic activity and selectivity were tested in the following reactions: cyclohexane dehydrogenation (reaction insensitive to structure), cyclopentane hydrogenolysis (reaction sensitive to structure) and carvone hydrogenation. The hydrogenation of carvone (a terpenic monocyclic ketone) is useful to analyze the selectivity of PtSn catalysts as carvone contains three different functional groups to be hydrogenated: one C=O group and two C=C bonds (one endocyclic and one exocyclic).

The present investigation focused on the relationships between the preparation procedure and support properties, the characteristics of the resulting catalysts, and the catalytic behavior.

2. Experimental

2. 1. Preparation of Catalysts

The supports were obtained from a peach pit-derived commercial activated carbon (GA-160 from Carbonac). The original carbon, crushed to 100-140 mesh, was purified by successive treatments with aqueous solutions (10 wt%) of HCl, HNO_3 and HF, followed by heat treatment in H_2 flow at 1123 K[10)]. After these treatments, the inorganic impurities decreased from 2.9 to 0.16 wt%. All sulfur compounds (poisons of noble metals) were eliminated. Purified carbon, named **C**, was oxidized by treatment with H_2O_2 aqueous solution (20 v/v%) at room temperature for 48 h[10)]. The H_2O_2-functionalized carbon was named **C–HP**.

Carbons **C** and **C–HP** had specific surface areas close to 900 m^2/g and a similar porous texture[10)]. The pH values of the aqueous suspensions of these supports were 10.5 and 6.5, respectively.

Two different impregnation sequences were used to prepare the PtSn/carbon samples: (a) coimpregnation (CI) with a HCl 0.4 M (1 M = 1 $mol \cdot dm^{-3}$) aqueous solution of H_2PtCl_6 and $SnCl_2$ and (b) two-step or successive impregnation (SI): first the carbon was impregnated with a HCl 0.4 M aqueous solution of $SnCl_2$, followed by drying at 393 K, and then impregnated with an aqueous solution of H_2PtCl_6. Pt/carbon and Sn/carbon samples were also prepared by impregnation. Impregnations, using 30 m*l* of solution per gram of carbon, were carried out by stirring the support with the solution at 298 K for 6 h. After filtration, the solid was dried at 393 K for 24 h. Concentrations of the impregnating solutions were appropriate to obtain about 1 wt% Pt, and a molar ratio Pt/Sn close to 1 (about 0.4 wt% Sn).

The catalysts were named PtSn/support (X), with support **C** or **C–HP**; and X=CI or SI, to identify the samples prepared by coimpregnation or successive impregnation, respectively. The platinum and tin loading, and the PtSn molar ratio of the different catalysts are shown in **Table 1**.

2. 2. TPD and TPR Experiments

Temperature-programmed experiments (TPD and TPR) were carried out using a differential flow reactor coupled to a mass spectrometer. Approximately 200 mg of sample was heated at 50 $K \cdot min^{-1}$ from room temperature up to about 1223 K under a gas flow (60 $ml \cdot min^{-1}$) of He for TPD experiments and H_2 (5 v/v%)–He for TPR measurements.

Table 1 Pt and Sn Loading, Pt/Sn Molar Ratio, and H/Pt Molar Ratio Determined from H_2 Chemisorption Measurements

Catalyst	wt% Pt	wt% Sn	Pt/Sn	H/Pt
Pt/C	0.85	—	—	0.39
Pt/C-HP	0.84	—	—	0.45
Sn/C	—	0.43	—	—
Sn/C-HP	—	0.45	—	—
PtSn/C(CI)	0.78	0.36	1.32	0.23
PtSn/C(SI)	0.86	0.42	1.25	0.28
PtSn/C-HP(CI)	0.81	0.38	1.30	0.24
Pt/C-HP(SI)	0.89	0.39	1.38	0.27

2. 3. XPS Analysis

XPS were obtained with a Fisons ESCALAB MkII 200R spectrometer, using a MgKα (1253.6 eV) source operated at 12 kV and 10 mA and a spherical electron analyser. The pressure of the analysis chamber was lower than 1.3×10^{-7} Pa. Peak areas were estimated from the integral after subtraction of the S-shaped background and Lorentzian–Gaussian fitting of the experimental peaks. Binding energies were referred to the C 1s peak at 284.9 eV. XPS measurements were carried out on both dried samples and samples previously treated *in-situ* with H_2 at 623 K for 4 h.

2. 4. H_2 Chemisorption

H_2 chemisorption measurements were carried out at 298 K in a volumetric equipment. Previously, the catalysts were reduced with H_2 (60 m*l*$\cdot$min^{-1}) at 623 K for 4 h and then outgassed (P = 0.013 Pa) at 623 K for 1 h.

2. 5. XAFS Measurements

The X-ray absorption experiments were performed at the BL-7C station of the Photon Factory in the National Laboratory for High Energy Physics (KEK-PF) in Tsukuba, Japan. A Si (111) double crystal was used to monochromatize the X-ray beam from the 2.5 GeV electron storage ring. The Pt L$_{III}$-edge absorption spectra were recorded in the transmission mode at room temperature, in a range of photon energy from 11,300 to 12,700 eV. Wafers for XAFS experiments were prepared by pressing a homogeneous mixture of the catalyst and polyethylene.

Measurements were carried out on dried and reduced samples (obtained by treatment in H_2 flow, 60 m*l*$\cdot$min^{-1}, at 623 K for 4 h). After the reduction treatment, samples were transferred, without exposure to air, to a glove box where the polyethylene wafers were prepared and vacuum-packed under an inert atmosphere. Pt foil, PtO_2 and H_2PtCl_6 were also analyzed as reference spectra.

Data analysis used Fourier transformation of the k^3-weighted EXAFS oscillations (range of 3-12 Å^{-1} (1 Å = 10^{-10} m)). The physical basis, data processing and numerous applications of XAFS spectroscopy have been reported elsewhere[22)~25)].

2. 6. Catalytic Activity Determination

Prior to any catalytic test, the catalysts were reduced *in-situ* with H_2 at 623 K for 4 h. The reactions were performed according to the conditions indicated below.

2. 6. 1. Cyclohexane Dehydrogenation and Cyclopentane Hydrogenolysis

Catalytic tests were performed at atmospheric pressure in a differential flow reactor using molar ratios of $H_2/C_6H_{12} = 29$ and $H_2/C_5H_{10} = 25$, and molar flow of 0.056 mol$\cdot$h^{-1} C_6H_{12} and 0.064 mol$\cdot$h^{-1} C_5H_{10}, for cyclohexane dehydrogenation and cyclopentane hydrogenolysis, respectively. For the first reaction, the activation energy was obtained by measuring the catalytic activity at 543, 558 and 573 K. The second reaction was carried out at 673 K.

In both cases, the mass of catalyst used was appropriate to obtain a hydrocarbon conversion lower than 7%. The progress of the reaction was followed by gas chromatography. Reaction products were benzene for cyclohexane dehydrogenation and pentane for cyclopentane hydrogenolysis.

2. 6. 2. Carvone Hydrogenation

This reaction was carried out at 313 K and atmospheric pressure in a discontinuous volumetric reaction equipment with a stirring rate of 360 rpm. The experiments used 0.09 g of carvone dissolved in 30 m*l* of toluene and 0.40 g of catalyst. Liquid samples were intermittently withdrawn from the reactor and analyzed by gas chromatography, using a capillary column Supelcowax 10 M.

3. Results and Discussion

3. 1. Chemistry of Impregnation of Carbon with Aqueous Solutions of Platinum and Tin Precursors

Impregnation of carbon materials with aqueous solution of H_2PtCl_6 takes place through a redox process between the platinum compound and the carbon surface[10),12),14),30),33),39)~42)]. As a consequence, after impregnation, the supported platinum has an oxidation state lower than Pt(IV). According to the mechanism proposed by van Dam and van Bekkum[39)], $[PtCl_6]^{2-}$ species is reduced to $[PtCl_4]^{2-}$ by the support. A reducing site on the carrier surface is denoted as C–H, with C–OH as the (acidic) oxidation product. The ionic Pt(II) species interacts, further or simultaneously, with a site S on the support surface, forming a $[PtCl_3S]^-$ species. Two possibilities for the nature of the ligand site S have been suggested[39)]: C=C structures in the carbon basal planes and oxygen-containing functional groups on the basal plane edges. Although identification of the exact structure of the complexes was not possible, ionic Pt^{II} formed during impregnation is probably bound at the basal plane edges[39)]. According to that model, most platinum should be present as

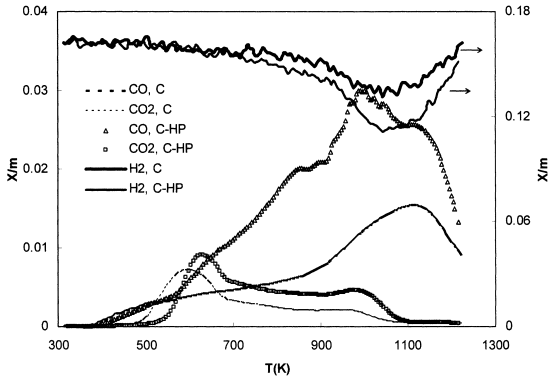

Fig. 1 CO, CO_2 and H_2 Profiles in the TPR Experiments (H_2(5 v/v%)–He, 20 K·min^{-1}) of Carbons **C** and **C–HP**

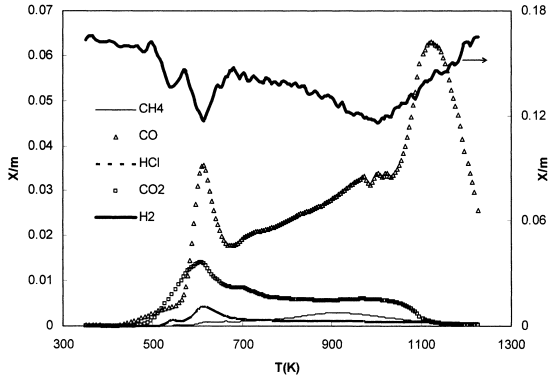

Fig. 2 CO, CO_2 H_2, CH_4 and HCl Profiles in the TPR Experiment (H_2(5 v/v%)–He, 20 K·min^{-1}) of **Pt/C–HP**

reduced Pt(II). However, Pt(IV) species were found[39], indicating reoxidation during the sample preparation, although continuous presence cannot be excluded[39]. Interestingly, evidence has also been found for the presence of zero valent platinum in dried monometallic[30),40),42)] and PtSn bimetallic catalysts[12].

In the case of preparation of carbon supported PtSn catalysts by co-impregnation with a HCl solution of H_2PtCl_6 and $SnCl_2$[10], the following redox reactions should also be considered[36]:

$$[PtCl_6]^{2-} + [SnCl_3]^- + Cl^- \longrightarrow [PtCl_4]^{2-} + [SnCl_6]^{2-} \quad (1)$$

$$[PtCl_4]^{2-} + 2[SnCl_3]^- \longrightarrow [PtCl_2(SnCl_3)_2]^{2-} + 2Cl^- \quad (2)$$

For a Pt/Sn molar ratio equal to 1, since $[SnCl_3]^-$ ion will be preferentially consumed in reaction (1), we can consider that the solution used for co-impregnation contains mainly $[PtCl_4]^{2-}$, $[SnCl_6]^{2-}$ and Cl^- anions, and only small amounts of the $[PtCl_2(SnCl_3)_2]^{2-}$ complex. Also, the presence of Cl^- ions may have some effect in the interaction of the platinum species with the carbon surface. In fact, addition of hydrochloric acid or potassium chloride to the H_2PtCl_6 solution decreased the adsorption strength of the platinum species on the carbon surface[39]. A possible explanation is that the chloride-containing Pt complexes are more stable[43] and so interaction of the $[PtCl_4]^{2-}$ ions with the S support sites might be hindered.

Another aspect to be considered is the charge of the carbon surface respective to that of the species in the solution used for impregnation[28]. The analysis requires comparison of the pH of the support aqueous suspension (pH_{SUSP}) and the pH of the impregnating solution (pH_{SOL}). In general terms, if $pH_{SOL} < pH_{SUSP}$, the surface is positively charged and adsorption of anions is favored. This is the case for the catalysts of this study. Because the solutions used for impregnation are quite acidic, with pH < 2, the surface charges of both supports were probably not greatly different.

3. 2. TPD and TPR Experiments

The evolution of CO and CO_2 during TPD experiments on carbons **C** and **C–HP** was (in μmol of gas (*STP*) per gram of sample) for carbon **C** 259 μmolCO/g and 91 μmolCO_2/g, and for carbon **C–HP** 663 μmolCO/g and 133 μmolCO_2/g. These results indicate that oxidation with H_2O_2 mainly increases the amount of surface oxygen complexes that decompose as CO.

Figure 1 shows the TPR profiles of carbons **C** and **C–HP**. Units of the y-axis (in all TPR figures) are molar fraction divided by the mass of sample used in the experiment. H_2 consumption, mainly between 773 and 1173 K, has been attributed to the interaction of H_2 with the reactive surface sites created by decomposition of functional groups (particularly those that evolve as CO)[31),44)], probably because it occurs at higher temperature. Thus, hydrogen consumption is higher for more oxidized supports. As previously reported[31),44)], the interaction of H_2 with the carbon surface modifies the evolution profiles of CO and CO_2 compared with the TPD experiment. The most outstanding observation was that the decomposition of groups that evolve as CO is noticeably shifted to lower temperatures.

Figure 2 shows the TPR profile of **Pt/C–HP**, in which three H_2 consumption zones can be clearly observed. This profile is qualitatively similar to that obtained for **Pt/C**. Hydrogen consumed in the low-temperature region (maximum at 538-543 K) is associated with the reduction of the deposited metal complex. The maximum of the H_2 consumption, at about 620 K, coincides with both the maximum of the low-temperature CO_2 desorption and with a well-defined CO desorption peak. It seems that hydrogen, probably dissociated by metallic Pt, is consumed by interaction with the reactive surface sites created by decomposition of some surface groups at this relatively low temperature. The sharp CO desorption at about 620 K was not observed in the TPR of the supports (**Fig. 1**), but was found in the TPD profiles obtained for dried **Pt/C** and

Pt/C–HP (not shown in the figure). This suggests that CO evolution at low temperature comes from the decomposition of surface oxygen groups created during the impregnation step and may be related to the redox process between the metal precursor and the carbon surface described above.

Figures 3 and **4** show the TPR profile obtained for

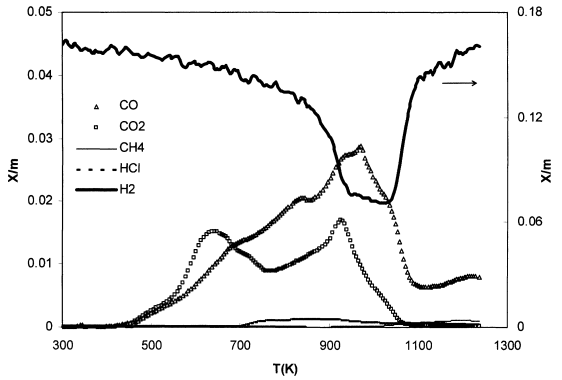

Fig. 3 CO, CO_2, H_2, CH_4 and HCl Profiles in the TPR Experiment (H_2(5 v/v%)–He, 20 K·min^{-1}) of **Sn/C–HP**

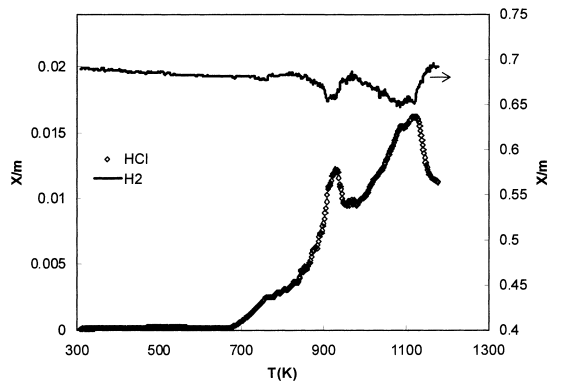

Fig. 4 H_2 and HCl Profiles in the TPR Experiment (H_2(5 v/v%)–He, 20 K·min^{-1}) of **$SnCl_2$**

Sn/C–HP and the analogous experiment carried out with bulk $SnCl_2$, respectively. The reduction of $SnCl_2$ occurs in two steps, revealed by hydrogen consumption at 923 K and 1073 K, accompanied by HCl desorption (**Fig. 4**). The H_2 consumption in the TPR of **Sn/C–HP** (**Fig. 3**) takes place in a broad zone, between 773 and 1123 K. A small and narrow HCl desorption peak was found between 773 and 873 K (not observed in the figure), indicating decomposition, and probable reduction, of the Sn chlorinated precursor at this temperature. The total amount of hydrogen consumed was about 28 mol H_2/mol Sn (the TPR profiles and the amount of H_2 consumed were similar for the **Sn/C** sample). This is much higher than the H_2 amount required for total reduction from Sn^{4+} (maximum oxidation state of Sn) to Sn^0 (2 mol H_2/mol Sn), indicating that hydrogen is retained on the carbon surface, probably related to the oxygen functionalities. To clarify this point, a TPR experiment was carried out with **Sn/C–HP** previously treated in He at 1173 K (conditions at which most of the surface oxygen groups are decomposed). In this case, the amount of H_2 consumed was much lower (about 3 mol H_2/mol Sn) and at 823-873 K. These results indicate that the presence of both metallic tin and surface functional groups determine the large retention of H_2 in **Sn/C** and **Sn/C–HP**.

Figures 5(a) and **5(b)** show the TPR profiles of **PtSn/C–HP(SI)** and **PtSn/C–HP(CI)**, respectively. The TPR profiles of the catalysts prepared with the non-oxidized support are very similar to those presented in **Fig. 5**. The main characteristic of these profiles is the well-defined hydrogen consumption between 473 and 773 K (divided into two peaks in the case of **PtSn/C–HP(CI)** (**Fig. 5(b)**). The amount of hydrogen consumed in this region is about 7 mol H_2/mol (Pt + Sn). However, since the maximum amount of hydrogen necessary for the total reduction of both metals (considering the presence of Pt(IV) and Sn(IV)) is 4 mol H_2/mol (Pt + Sn), some H_2 must have

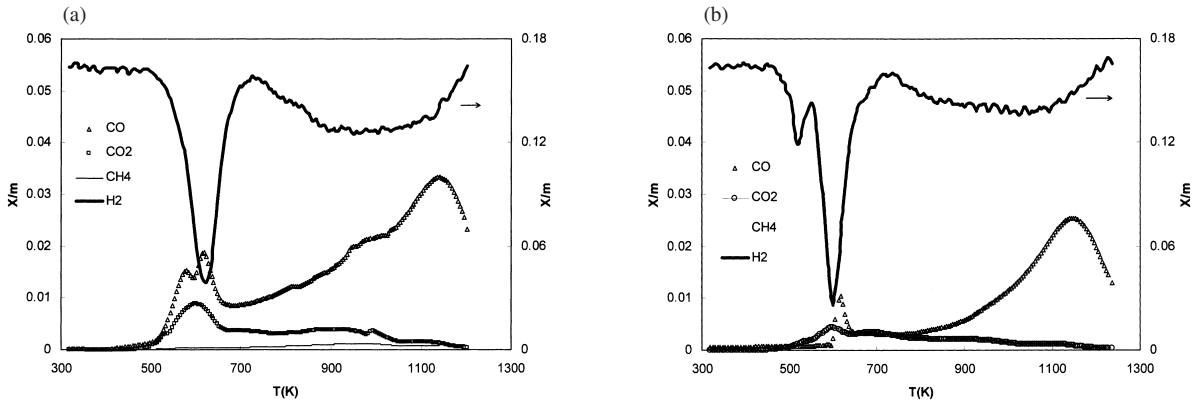

Fig. 5 CO, CO_2, H_2 and CH_4 Profiles in the TPR Experiment (H_2(5 v/v%)–He, 20 K·min^{-1}) of (a) **PtSn/C–HP(SI)** and (b) **PtSn/C–HP(CI)**

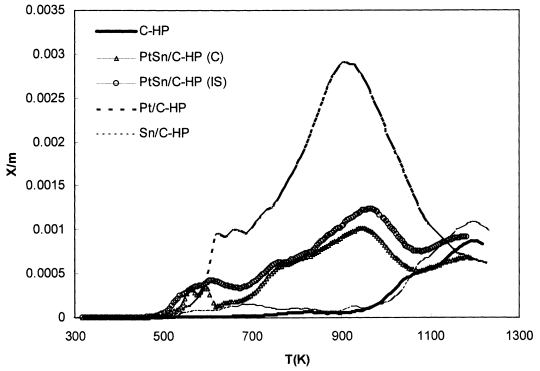

Fig. 6 CH_4 Profiles in the TPR Experiments (H_2(5 v/v%)–He, 20 K·min^{-1}) of Support **C–HP**, and the Monometallic and Bimetallic Catalysts Supported on Carbon **C–HP**

been retained on the carbon surface. Thus, tin is apparently reduced at lower temperature due to the presence of platinum in these catalysts, and some hydrogen is retained on the carbon surface below 673 K. Also, some H_2 consumption occurred between 773 and 1223 K (**Figs. 5(a)** and **5(b)**), which is quantitatively close to that observed in the same region of the TPR profiles of the supports and monometallic platinum. However, this is much lower than the H_2 consumption observed for **Sn/C** and **Sn/C–HP**.

The TPR profiles presented in **Fig. 5** also show a CO desorption peak at low temperature (523-673 K). As discussed above, this effect may be related to the presence of some surface groups formed during the impregnation. The area of this peak is lower in the catalysts prepared by coimpregnation (it is also observed in **PtSn/C(CI)**), which confirms that the interaction of the platinum species with the carbon surface is different depending on the impregnation procedure.

Formation of methane was also observed during the TPR experiments, and the obtained profiles are compared in **Fig. 6**. A small amount of methane was formed at 1073 K from **C–HP** and **Sn/C–HP** (8 and 11 μmol/g, respectively). Methane evolution reached a maximum at 923 K and was quantitatively much higher for **Pt/C–HP** (41 μmol/g). Methane formation was significant for the bimetallic samples (23 and 18 μmol/g for the (SI) and (CI) catalysts, respectively) at a slightly higher temperature (973 K). These results clearly indicate the catalytic effect of Pt on methane formation by support gasification. Addition of tin modified platinum to reduce its catalytic activity for methane formation. This modification was slightly greater for CI catalysts.

In summary, the TPR experiments revealed a close proximity between Pt and Sn in the bimetallic catalysts based on the easier reducibility of tin in PtSn samples, compared to Sn/carbon, and the lower methane formation with the PtSn catalysts compared to the monometallic Pt catalysts. The SI and CI methods affected the creation or modification of oxygen groups on the carbon surface in a different way. The profiles of CO and CO_2 evolution were quite similar for the two catalysts prepared by the same method, and different for catalysts prepared by a different impregnation procedure (for the catalysts prepared by SI, the evolution of CO and CO_2 was larger). Therefore, the impregnation solution produces a higher oxidation of the carbon surface and/or the metallic phase created after reduction favors the desorption of surface groups. The former proposal is in agreement with the model and conditions suggested by van Dam and van Bekkum[39] for the reduction of the platinum precursor by the support. In the CI procedure, reduction takes place by reaction of $[PtCl_6]^{2-}$ with the tin precursor in solution, and the interaction of $[PtCl_4]^{2-}$ with carbon is partially hindered because of the hydrochloric acid. Finally, the profiles of CH_4 evolution indicate that the modification of the catalytic properties of Pt by Sn is slightly greater for the CI samples. The TPR spectra did not show important differences between the catalysts related to the surface chemistry of the support.

3. 3. XPS Analysis

Table 2 shows the binding energies for Pt $4f_{7/2}$ and Sn $3d_{5/2}$ in **PtSn/C(CI)**, **PtSn/C(SI)**, **PtSn/C–HP(CI)**, and **PtSn/C–HP(SI)**, after drying and after the reduction treatment at 623 K. The Pt $4f_{7/2}$ binding energies of monometallic **Pt/C** and **Pt/C–HP** are also included. The deconvolution of the Pt $4f_{7/2}$ XPS spectra of dried samples reveals two peaks at 72.0-72.3 eV, and 73.5-73.9 eV; the relative amount of Pt in each of these two states is shown in **Table 2** as a percentage. The binding energy of Pt $4f_{7/2}$ in the reduced catalysts ranged from 71.7 to 71.9 eV.

By comparing with the binding energy values[45] for Pt $4f_{7/2}$: Pt^0 71.0-71.3 eV, $K_2Pt^{II}Cl_4$ 72.8-73.4 eV and $K_2Pt^{IV}Cl_6$ 74.1-74.3 eV; we observe that the reduced samples contain metallic Pt but with a binding energy slightly higher than that for Pt^0. This could be related to the interaction of Pt with a more electronegative atom or, in the case of bimetallic samples, to a modification of the electronic structure of platinum because a PtSn alloy is formed. A binding energy of 71.9 eV for the reduced monometallic **Pt/C** and **Pt/C–HP** reveals that the effect of the support is probably more important than the potential presence of a PtSn alloy.

Binding energies close to 72.0 eV were also found for reduced PtSn catalysts supported on carbon black[12] and carbon cloth[14], prepared in the same conditions. The binding energy for monometallic Pt/carbon catalyst was 71.5 eV[12], indicating that in this case the effect of the support was lower.

In the case of the dried catalysts, the assignment is more complicated because the observed binding ener-

Table 2 XPS Results: Pt $4f_{7/2}$ and Sn $3d_{5/2}$ Binding Energies, and Sn/Pt Surface Ratio in Reduced Samples

Sample	B.E. Pt $4f_{7/2}$ [eV]		B.E. Sn $3d_{5/2}$ [eV]		Sn/Pt atomic surface ratio
	Dried	Reduced	Dried	Reduced	
Pt/C	72.1 (60%)	71.9	—	—	—
	73.7 (40%)				
Pt/C–HP	72.3 (53%)	71.9	—	—	—
	73.8 (47%)				
PtSn/C(CI)	72.0 (54%)	71.8		486.4 (17%)	16.1
	73.7 (46%)		487.7	487.7 (83%)	
PtSn/C(SI)	72.0 (62%)	71.8		486.5 (12%)	24.4
	73.9 (38%)		487.7	487.8 (88%)	
PtSn/C–HP(CI)	72.1 (53%)	71.7		486.3 (14%)	23.3
	73.9 (47%)		487.8	487.7 (86%)	
PtSn/C–HP(SI)	72.0 (57%)	71.9		486.4 (14%)	27.0
	73.5 (43%)		487.8	487.7 (86%)	

gies did not agree with the published values[45]. In any case, it seems that there were two different species: one with oxidation state close to zero and the other one close to (Ⅱ). The existence of these two states, in similar proportions, is observed in both monometallic and bimetallic catalysts. For the carbon cloth supported PtSn system[14], platinum in the dried samples shows only one oxidation state with binding energy of 72.8 eV assigned to Pt(Ⅱ), whereas on the carbon black[12] two oxidation states with binding energy of 72.1 eV and 74.3 eV are observed. Our and previous results confirm that the reduction of platinum takes place during impregnation of the carbon supports.

The Sn $3d_{5/2}$ XPS spectra of the dried samples show a peak at 487.7-487.8 eV corresponding to Sn(Ⅱ) and/or Sn(Ⅳ) species (not distinguishable[46]), probably forming chlorinated compounds (**Table 2**). In the case of catalysts submitted to the reduction treatment, the Sn $3d_{5/2}$ spectrum shows two peaks: a main one at 487.7 eV corresponding to Sn(Ⅱ) and/or Sn(Ⅳ) species, and a weaker one at 486.3-486.5 eV, characteristic of metallic tin[45]. According to the relative intensities of these two peaks, the percentage of zero valent tin ranges between 12 and 17% of the total tin species. In carbon black supported PtSn[12], the amount of reduced tin was about 30%, while when a carbon cloth is used as support, reduction of tin is about 70%[14].

The atomic surface Sn/Pt ratios (**Table 2**) range between 16 and 27, revealing very important surface enrichment by tin. Such enrichment, although not so great, has also been found in other similar systems. For example, a Sn/Pt atomic surface ratio of 13 has been found for PtSn supported on a carbon cloth[14], a ratio of 2.5 has been observed in PtSn supported on carbon black[12] and also a low ratio, close to 3, was observed in PtSn catalysts supported on Al_2O_3[15].

The XPS results can be summarized as follows:

(1) The platinum precursor H_2PtCl_6 becomes reduced after the impregnation and drying steps, and platinum is present in two different oxidation states. Reduction of the tin precursor seems not to take place. The four bimetallic dried catalysts give similar results, although the amount of platinum in the most reduced state (close to zero) is slightly higher in the SI samples.

(2) After the reduction treatment, platinum is in the zero valent state but slightly electron deficient and tin is only partially reduced. High surface enrichment by tin is observed. The four bimetallic reduced catalysts show similar results but the amount of Sn^0 is slightly higher and tin enrichment slightly lower for the SI samples. The surface of the bimetallic catalysts consists of metallic platinum (interacting with other elements), a major fraction of tin as Sn(Ⅱ) and/or Sn(Ⅳ) species, and a relatively small amount of Sn^0, which could be alloyed with Pt.

(3) XPS of the four bimetallic catalysts, either dried or reduced, revealed a greater similarity between the samples prepared with the oxidized support, **C–HP**, than between those prepared with the original carbon support, **C**.

3. 4. H_2 Chemisorption Measurements

The molar H/Pt ratio obtained for the mono- and bimetallic catalysts is shown in **Table 1**. The chemisorption capacity indicated the following trend:

Pt/C–HP > Pt/C > PtSn/C(SI) > PtSn/C–HP(SI) > PtSn/C(CI) ≈ PtSn/C–HP(CI)

As expected, the addition of tin to platinum decreased the chemisorption capacity, probably due to both electronic and geometric effects. This decrease was less pronounced than in other reported systems. For example, the H/Pt ratio was 0.15 for a PtSn catalyst (Pt/Sn = 1.22) prepared by successive impregnation of a pregraphitized carbon black, in contrast to 0.92 for the monometallic Pt catalyst[12]. However, 30% of tin was reduced after treatment with H_2 at 623 K. The chemisorptive capacity of $PtSn/Al_2O_3$ catalysts decreased from H/Pt = 1 in the monometallic catalyst to about 0.15 in the bimetallic catalyst[33]. More recently, with $PdSn/SiO_2$ prepared by the "solvated metal atom dispersed" method, a strong decrease in the H/Pd ratio

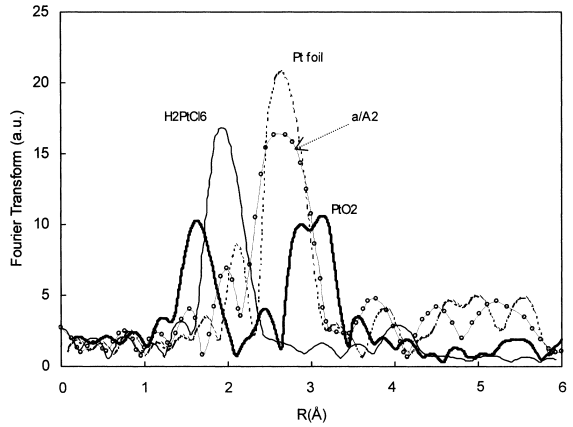

Fig. 7 FT-EXAFS Profiles of the Reference Compounds H_2PtCl_6, PtO_2 and Pt Foil, and Sample a/A2 (see the text for description)

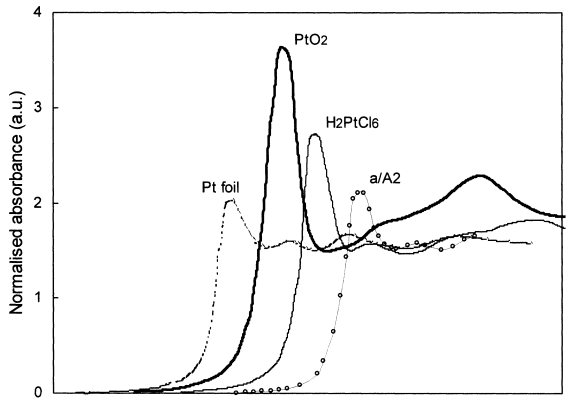

Fig. 8 XANES Profiles of the Reference Compounds H_2PtCl_6, PtO_2 and Pt Foil, and Sample a/A2 (see the text for description)

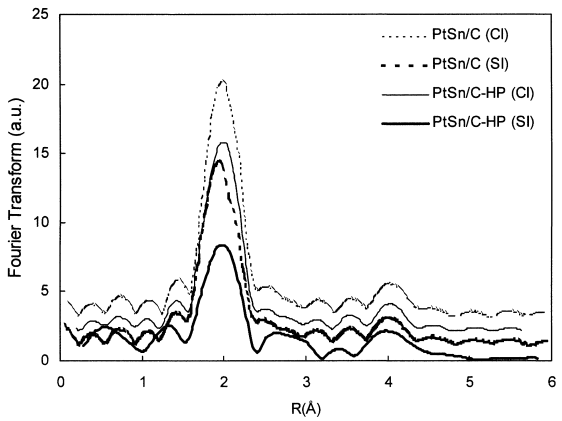

Fig. 9 FT-EXAFS Profiles of the Dried Bimetallic Samples **PtSn/C(CI)**, **PtSn/C(SI)**, **PtSn/C-HP(CI)** and **PtSn/C-HP(SI)**

was found (10 times lower than for Pd/SiO_2), but, surprisingly, no loss in H_2 chemisorption capacity for $PdSn/Al_2O_3$[26] was observed.

In the catalysts subject of the present work, the decrease in the chemisorption capacity appeared to be higher in catalysts prepared by coimpregnation. In this case, there is probably more intimate contact between the metals that could lead to an easier formation of alloy during thermal treatments. This is in agreement with the higher modification of Pt by Sn in the **PtSn/C-HP(CI)**, compared to the analogous **PtSn/C-HP(SI)**, as observed by the TPR-methane evolution

3. 5. XAFS Analysis

3. 5. 1. Reference Compounds

The FT-EXAFS and XANES (X-ray absorption near edge structure) profiles of the reference compounds H_2PtCl_6, PtO_2, and Pt foil are presented in **Figs. 7** and **8**, respectively. Results corresponding to a reduced Pt/carbon catalyst with a low platinum dispersion (about 20%, corresponding to a particle size close to 5 nm)[30] labeled as a/A2 have been also included. Platinum particles of about 5 nm exhibit a structure similar to that of bulk metal but without the problems related to thickness[47),48)], and so they are more useful for XAFS studies. As observed in **Figs. 7** and **8**, the XAFS signals of the platinum foil and the a/A2 catalyst contain the same general features. The distances used in the following discussion are those directly observed in the FT-EXAFS data; that is, without phase-shift correction.

3. 5. 2. Dried Samples

The FT-EXAFS profiles of the dried samples **PtSn/C(CI)**, **PtSn/C(SI)**, **PtSn/C-HP(CI)** and **PtSn/C-HP(SI)**, shown in **Fig. 9**, are characterized by a main peak located at about 2 Å. The differences between the four spectra are mainly related to the intensity of this peak. Comparing these spectra with the FT-EXAFS profile of the reference compound H_2PtCl_6 (**Fig. 7**) indicates that the peak located at about 2 Å is likely due to Pt–Cl bonds. A decrease in the intensity of that peak should be related to a reduction in the coordination of platinum by Cl or to the substitution of this ligand by lighter scatterers[11),22)~25),30)]. In fact, taking into account the chemistry of the impregnation of carbon with H_2PtCl_6 aqueous solutions, the chloride coordination of platinum decreases due to the interaction of platinum with oxygen or carbon atoms on the support.

The FT-EXAFS profiles shown in **Fig. 9** do not reveal the presence of Pt–Sn and Pt–Pt interactions. The Pt–Sn distance in an alloy is about 2.7 Å[21),49)] and about 2.5 Å in the $[Pt(SnCl_3)_5]^{3-}$ complex[50)]. The absence of a Pt–Sn interaction can also be deduced because of the great similarity with the FT-EXAFS profiles obtained for the monometallic **Pt/C** and **Pt/C-HP** catalysts[11)]. On the other hand, comparing the results

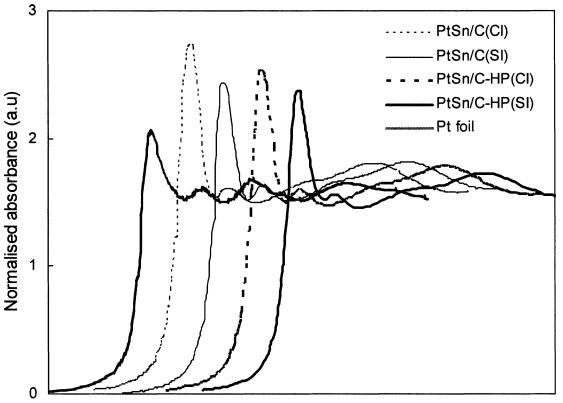

Fig. 10 XANES Profiles of the Dried Bimetallic Samples **PtSn/C(CI)**, **PtSn/C(SI)**, **PtSn/C–HP(CI)** and **PtSn/C–HP(SI)**, and Pt Foil

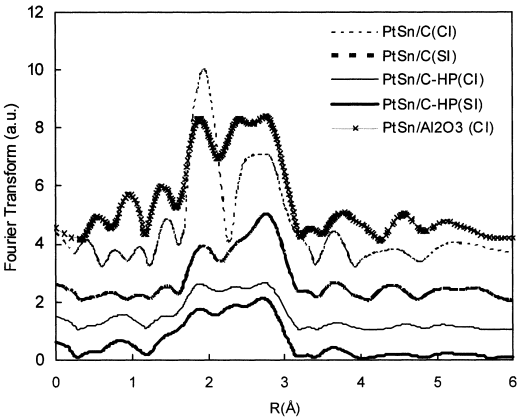

Fig. 11 FT-EXAFS Profiles of the Reduced Bimetallic Samples **PtSn/C(CI)**, **PtSn/C(SI)**, **PtSn/C–HP(CI)**, **PtSn/C–HP(SI)** and **PtSn/Al_2O_3(CI)**

obtained with catalysts prepared on carbons **C** and **C–HP**, the effect of the support surface chemistry on the state of platinum can be deduced. In catalysts prepared with the oxidized support (**C–HP**), the intensity of the main peak is lower than in catalysts prepared with carbon **C**. This effect was also observed with the monometallic Pt/carbon samples[11]. These results can be explained by a higher coordination of Pt with O and/or C atoms in the oxidized support. Therefore, the interaction of the platinum species with the support is more extensive with the oxidized surface, independent of both the presence of tin and the impregnation procedure.

Comparison of the FT-EXAFS profiles of **PtSn/C(CI)** and **PtSn/C(SI)**, and **PtSn/C–HP(CI)** and **PtSn/C–HP(SI)** (**Fig. 9**) shows that the intensity of the main peak (close to 2 Å) is lower for the catalysts prepared by successive impregnation. In this case, the platinum species interact more effectively with the surface of the support. The effect of the preparation method can be explained by considering that during co-impregnation (in a HCl 0.4 M solution), the presence of Cl^- ions increases the stability of the chloride-containing Pt complexes[43]. Therefore, the adsorption of the platinum species on the carbon surface is lower and the loss of chloride ligands is hindered.

The absorption edges corresponding to the four bimetallic dried catalysts and the platinum foil are plotted in **Fig. 10**. Taking the data for Pt foil as a reference, these results indicate that a noticeable concentration of vacant d-electron states in the dried samples. The intensity of the white line decreased in the following order:

PtSn/C(CI) > PtSn/C–HP(CI) > PtSn/C(SI) > PtSn/C–HP(SI)

These results also reveal the effect of the surface oxidation of the support. For a given preparation method, platinum atoms in catalysts prepared with non-oxidized support are more electron deficient (*i.e.*, the intensity of the white line is higher). Comparing samples prepared with the same support, platinum is more electron deficient in catalysts prepared by co-impregnation. The higher electron deficiency may be related to a weaker interaction of Pt species with the support that results in less reduction of platinum by contact with carbon. This interpretation agrees with the EXAFS data discussed above. No significant differences were observed in the energy of the peak top of the white line (appearing at about 11,560 eV).

Comparison of the absorption edge between bimetallic and monometallic catalysts indicates that the electronic state of platinum in the dried samples is not highly modified by tin addition. As previously reported[30], the intensity of the white line for the monometallic catalysts is intermediate between those corresponding to the bimetallic catalysts; both for catalysts prepared with the original carbon or with the oxidized carbon.

In summary, the FT-EXAFS profiles (**Fig. 9**) and the intensity of the white line (**Fig. 10**) of the analyzed catalysts show that oxidation of the support surface favors the removal of Cl from the coordination sphere of platinum. Also, the conditions used in the co-impregnation method hinder the interaction of the platinum species with the carbon surface. The XAFS results obtained for dried bimetallic catalysts did not reveal any chemical interaction between Pt and Sn. However, the results of the TPR experiments suggest that both metals are in relatively close proximity.

3. 5. 3. Reduced Samples

XPS showed that platinum was fully reduced (but with some electron deficiency) after the reducing treatment (H_2, 623 K, 4 h) in the four bimetallic catalysts supported on carbon. However, the FT-EXAFS profiles (**Fig. 11**) showed significant differences in the coordination of platinum in these four catalysts. The data obtained for the **PtSn/Al_2O_3(CI)** catalyst are also

included in **Fig. 11**. The FT-EXAFS profiles of the reduced samples show three main peaks (not completely resolved) with different relative intensities. The three peaks are located at the following distance ranges (without phase-shift correction): 1.85-2.10 Å, 2.35-2.50 Å and 2.65-2.80 Å. FT-EXAFS of bimetallic PtSn catalysts supported on Al_2O_3[20),51)], graphite[49)] and SiO_2[16),52)] showed profiles with three main peaks at similar distance ranges. The previous[16),20),49)~52)] and present FT-EXAFS spectra indicate that the signals observed in the range from 2.35 to 2.80 Å in **Fig. 11** could be due to Pt–Sn and/or Pt–Pt interactions.

According to several authors[49)~52)], the Pt–Pt bond contributes to the larger distance range of the FT-EXAFS profile (at about 2.77 Å) whereas the contribution of the Pt–Sn bond appears at slightly lower distances (depending on the formed PtSn species). Ramallo *et al.*[16)] also report that the Pt–Sn distance is slightly lower than the Pt–Pt distance (2.68 *versus* 2.71 Å). However, in the work of Caballero *et al.*[20)] a peak at 2.68 Å was assigned to the Pt–Pt bond and a peak at 2.93 Å to the Pt–Sn bond. There is also disagreement about the assignation of the peak at lower distances (< 2.10 Å). This peak has been assigned to the interaction of platinum clusters with the support *via* Pt–O–Sn^{2+} species[20)], not clearly defined[49)], explained as an interference phenomenon between the Pt–Pt and Pt–Sn bonds[21),52)], and as a Pt–O interaction at 1.99 Å related to interaction with the SiO_2 support[16)]. These discrepancies reveal the difficulty in accurate quantification of the EXAFS oscillations and show that the use of appropriate references and complementary techniques is necessary for the correct assessment of bond distances and co-ordination numbers.

To justify the interaction of tin and platinum found in TPR experiments, we suggest that the FT-EXAFS signals observed below 2.10 Å originate from Pt–O–Sn^{2+} species.

The FT-EXAFS profiles obtained for catalysts prepared with the oxidized support (*i.e.*, **PtSn/C–HP(CI)** and **PtSn/C–HP(SI)**) (**Fig. 11**) are very similar, with the three above-mentioned maxima and the same relative intensity. This suggests that the preparation method does not cause significant differences in the state of the reduced platinum. It is interesting to emphasize that the three peaks found in the FT-EXAFS spectrum of the **PtSn/Al_2O_3(CI)** catalyst also had similar relative intensity.

On the other hand, for catalysts prepared with support **C**, the peak at lower distances (from 1.85 to 2.10 Å in **Fig. 11**) was more intense, and better defined and resolved for **PtSn/C(CI)** than for **PtSn/C(SI)**. According to the criteria explained above, this means that the interaction of metallic platinum with the support (as Pt–C or Pt–O) or with tin through the Pt–O–Sn^{2+} species is higher in the catalyst **PtSn/C(CI)**.

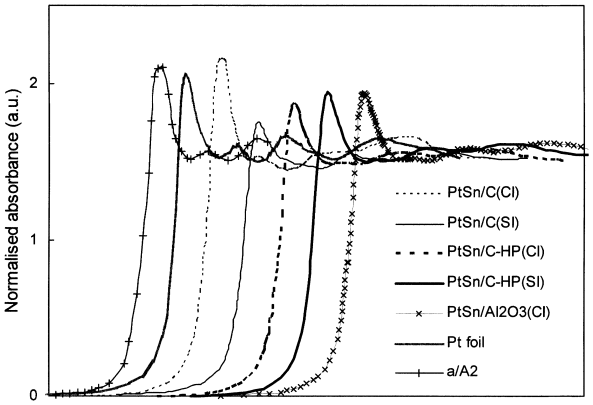

Fig. 12 XANES Profiles of the Reduced Samples **PtSn/C(CI)**, **PtSn/C(SI)**, **PtSn/C–HP(CI)**, **PtSn/C–HP(SI)** and **PtSn/Al_2O_3(CI)**, and a/A2 and Pt Foil

Considering that the interaction of platinum species with the support is less extensive for the dried **PtSn/C(CI)** sample than for the analogous SI sample, an important effect of the reduction treatment is inferred.

The analysis of the Pt L_{III} absorption edge can give us some additional information about the electronic state of platinum. **Figure 12** shows this part of the XAFS spectrum for the four PtSn catalysts supported on carbon, the **PtSn/Al_2O_3(CI)** catalyst, platinum foil and sample a/A2. The intensity of the white line for the different samples increased in the following order:

PtSn/C(SI) < **PtSn/Al_2O_3(CI)** ≈ **PtSn/C–HP(CI)** ≈ **PtSn/C–HP(SI)** < Pt foil < a/A2 < **PtSn/C(CI)**

Platinum had the most electron deficient state in **PtSn/C(CI)**. This result agrees with the largest interaction of Pt with electronegative atoms like O (for example through Pt–O–Sn^{2+} species or with the support) in this catalyst. The electronic state of platinum is similar in **PtSn/C–HP(CI)**, **PtSn/C–HP(SI)**, and **PtSn/Al_2O_3(CI)**. This observation could be related to the similar intensities of the main peaks of the FT-EXAFS profiles for these three catalysts (**Fig. 11**). The intensity of the white line in these catalysts and in **PtSn/C(SI)** is lower than that in platinum foil and in the reference sample a/A2. A similar result was previously observed in a PtSn/Al_2O_3 catalyst[20)]. This effect is explained by the formation of a Pt–Sn alloy resulting in increased d-electron density of platinum atoms. Thus, the results shown in **Fig. 12** suggest that the **PtSn/C(SI)** catalyst contains the largest amount of PtSn alloy. Additionally, a PtSn bimetallic phase was likely to be formed to a similar extent in **PtSn/C–HP(CI)**, **PtSn/C–HP(SI)**, and **PtSn/Al_2O_3(CI)**. The oxygen groups on the surface of Al_2O_3 apparently have an effect similar to that of surface oxygen functionalities on the carbon support.

In summary, the surface chemistry of the carbon sup-

Table 3 Catalytic Activity in Test Reactions and Activation Energy (E_a) for CHD

Catalyst	CPH	CHD		
	rate [mol·h^{-1}·g$_{pt}^{-1}$]	rate [mol·h^{-1}·g$_{pt}^{-1}$]	TOF	E_a [kJ/mol]
PtSn/C(CI)	0	2.2	—	29.4
PtSn/C(SI)	0	3.0	—	28.8
PtSn/C-HP(CI)	0	9.9	—	30.1
PtSn/C-HP(SI)	0	7.7	—	26.1
PtSn/Al_2O_3	0	12.1	—	30.0
Pt/C	1.7	32.0	82	19.6
Pt/C-HP	2.0	86.2	192	21.6

port and the preparation method of the catalysts influence the structure of the metallic particles in the reduced catalysts. With an oxidized support, both preparation methods (CI and SI) will produce a similar structure, close to the structure of PtSn catalysts supported on Al_2O_3. On the other hand, the non-oxidized support will produce a different structure of the metallic phase depending on the impregnation procedure.

3. 6. Catalytic Activity in the Test Reactions

The initial catalytic activities (expressed as reaction rate in mol/h g Pt) for cyclohexane dehydrogenation (CHD) and cyclopentane hydrogenolysis (CPH) with the monometallic and bimetallic carbon-supported catalysts are presented in **Table 3**. In the case of CHD, activation energy (E_a) and turnover frequency (TOF) of the monometallic catalysts have been also included.

Addition of tin results in an important decrease of the rate of both reactions, being the activity for CPH suppressed. The activation energies in CHD for the bimetallic catalysts are noticeably higher than those for the monometallic samples. This effect can be attributed to the electronic modification of platinum by tin in the reduced bimetallic catalysts. **Table 3** also reveals the clear effect of the support surface chemistry for both monometallic and bimetallic catalysts, with greater activity in the catalysts prepared with oxidized carbon. The different impregnation procedure (in the case of bimetallic catalysts) does not produce noticeable differences in the catalytic activity.

The lack of activity of the bimetallic catalysts for CPH indicates that the cluster structures of Pt atoms required for this reaction are not formed or are not accessible to the reactants. That is, tin must have produced dilution and/or blockage of the Pt particles. The large tin surface enrichment determined by XPS (**Table 2**) may be considered as evidence of the blocking effect.

Cyclohexane dehydrogenation is a structure-insensitive reaction, so similar TOF values should have been obtained for both monometallic catalysts. However, **Pt/C** and **Pt/C-HP** catalysts show different TOF. This effect has been previously observed in a series of catalysts prepared with carbon supports of different surface chemistry[32], and is related to the location and accessibility of platinum particles. In the case of **Pt/C** and **Pt/C-HP**, due to the interaction with the surface oxygen groups of the support, platinum is considered to be more externally located on the oxidized support and thus is more accessible to reactants. With the non-oxidized support, a fraction of the platinum can be anchored in a region accessible to hydrogen but not to the more voluminous cyclohexane molecule. Therefore, not all active sites determined by hydrogen chemisorption are actually active for cyclohexane dehydrogenation.

The differences between the catalytic activity of bimetallic catalysts prepared with oxidized and non-oxidized supports can also be explained by these arguments. Catalysts prepared with the oxidized support and with alumina had relatively close catalytic activity, in agreement with the similar structure and electronic state of platinum deduced from the XAFS data. On the other hand, **PtSn/C(CI)** and **PtSn/C(SI)**, both with low and similar catalytic activity, have different metallic structure and electronic state of platinum, according to the XAFS analysis. In this case, the above-suggested accessibility of the reactants to the active metallic species may be the major factor responsible for the low catalytic activity.

3. 7. Hydrogenation of Carvone

Hydrogenation of carvone can be described by the reaction scheme shown in **Scheme 1**. The selective hydrogenation of one or both of the double bonds C=C produces unsaturated or saturated ketones, respectively. The selective hydrogenation of the C=O group produces unsaturated alcohols, which are more valuable products. The hydrogenation could continue to the saturated alcohol.

Considering the thermodynamics of the hydrogenation of the two functionalities and the specific adsorption sites for each[4], the analysis of the catalytic properties could be helpful to infer the presence of particular catalytic structures in PtSn catalysts.

Figure 13 shows the carvone conversion *versus* reaction time obtained with **Pt/C-HP**, **PtSn/C-HP(CI)** and **PtSn/C-HP(SI)**. As expected, tin addition pro-

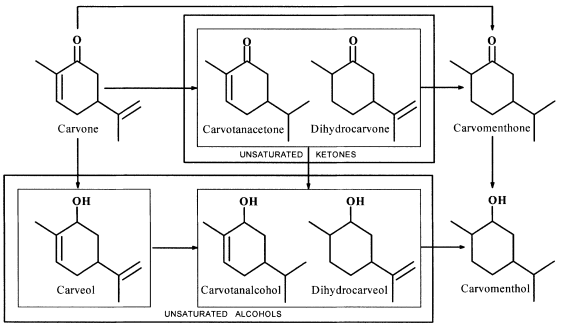

Scheme 1 Possible Products from Carvone Hydrogenation

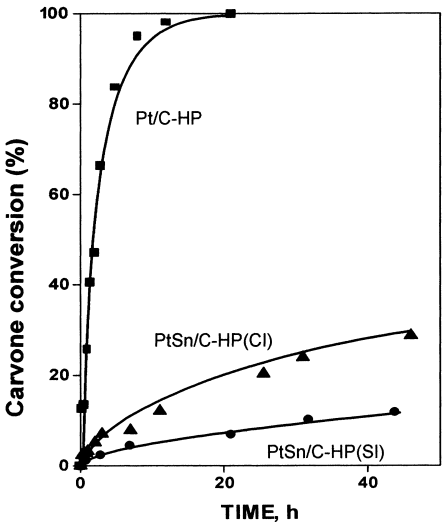

Fig. 13 Carvone Conversion *vs.* Time with Catalysts **Pt/C-HP**, **PtSn/C-HP(CI)** and **PtSn/C-HP(SI)**

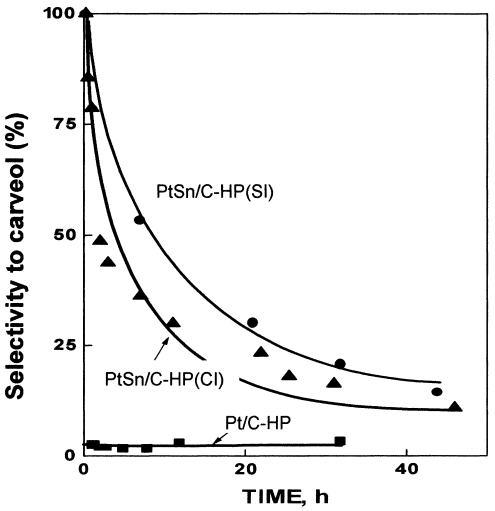

Fig. 14 Selectivity to Carveol *vs.* Time with Catalysts **Pt/C-HP**, **PtSn/C-HP(CI)** and **PtSn/C-HP(SI)**

duces a noticeable decrease in the catalytic activity. The bimetallic PtSn catalyst prepared by co-impregnation is more active.

The products detected were only unsaturated ketones (mainly carvotanacetone) and unsaturated alcohols (mainly carveol, the doubly unsaturated alcohol), see **Scheme 1**. **Figure 14** shows the selectivity to unsaturated alcohols as a function of the reaction time. **Pt/C-HP** is very selective for unsaturated ketones over the whole range of the reaction time (96% unsaturated ketones for the total conversion of carvone), and as a consequence the selectivity for unsaturated alcohols is very low (about 3-4%). As shown in **Fig. 14**, the selectivity of the carbon-supported Pt catalyst for unsaturated alcohols (mainly carveol) is substantially enhanced by tin addition and is slightly higher for the catalyst prepared by successive impregnation (less active catalyst).

The selectivity of PtSn catalysts for unsaturated alcohols is very high at low reaction times, reaching values close to 100 at the beginning of the reaction, but decreases with time because the production of carvotanacetone increases. Both carveol (the doubly unsaturated alcohol) and carvotanacetone are produced from direct hydrogenation of carvone, not as a product of a consecutive reaction (**Scheme 1**).

The noticeable selectivity for the unsaturated alcohols shown by the catalysts in this study has not been observed in previous research dealing with carvone hydrogenation[19),37),53)~55)]. As an example, **Table 4** shows the product distribution, at a total conversion of carvone, obtained with different monometallic and bimetallic catalysts. Comparison of the results obtained with monometallic Pt on different supports reveals a very important effect of the support on the selectivity of the catalysts. If carbon is used as support, further hydrogenation of the unsaturated ketones (mainly carvotanacetone) is strongly decreased. In the case of Pt and Pd supported on inorganic oxides, the selectivity for saturated ketones has been interpreted according to the size and crystalline structure of the metal particles. In general, the adsorption of carvotanacetone is stronger on small particles, leading to the reduction of the exocyclic double bond prior to desorption[54),55)]. Considering the H_2 chemisorption capacity as an approximation to the particle size, (H/M ratio in **Table 4**), the above discussion can explain the differences in the selectivity of Pt/Al_2O_3 and Pt/SiO_2 shown in **Table 4**. In the case of the carbon-supported catalyst, an additional effect related to the support should be considered. That is, the carbon support may increase the electronic density of the adsorption sites, leading to weaker adsorption of carvotanacetone.

The addition of tin to noble metal, in comparison to other metals like Cu[54)] or Au[55)], favors the production of alcohols (see **Table 4**). This effect is more pro-

Table 4 Product Distribution of Different Catalysts in the Hydrogenation of Carvone

Catalyst	UK	UA	SK	SA	H/M[f] (M = Pt, Pd) [mol/mol]	M_s/M_a[g]	Ref.
Pt/C–HP	96	2	1	0	0.45	—	19, 10
Pt/Al_2O_3	10	0	90	0	1.00	—	19, 37
PtSn/Al_2O_3(SI)	34	1	56	8	0.15	0.65	19, 37
PtSn/Al_2O_3(CI)	43	4	36	17	0.13	0.65	19, 37
Pt/SiO_2[a]	31	—	69	—	0.48	—	54
PtAu/SiO_2[b]	58	—	42	—	0.32	0.13	54
Pd/SiO_2[c]	64	—	36	—	0.54	—	55
PdCu/SiO_2(SR)[d]	73	—	27	—	0.33	0.17	55
PdCu/SiO_2(CI)[e]	32	—	68	—	0.46	0.55	55

UK: unsaturated ketones, UA: unsaturated alcohols, SK: saturated ketones, SA: saturated alcohols.
a) 6 wt% Pt.
b) 6 wt% Pt and 0.8 wt% Au.
c) 1.46 wt% Pd.
d) SR = surface redox reaction, 1.42 wt% Pd and 0.14 wt% Cu.
e) CI = coimpregnation, 0.85 wt% Pd and 0.28 wt% Cu.
f) from H_2 chemisorption.
g) second metal to active metal molar ratio.

nounced in the case of carbon-supported catalysts (**Fig. 14**). Taking into account the H_2-chemisorption capacity of carbon-supported PtSn catalysts (**Table 1**), we can suggest an important effect of the carbon support. However, the differences in the state of tin between carbon and alumina supported PtSn catalysts must also be considered. As revealed by XPS analysis: (i) the amount of Sn (Ⅱ, Ⅳ) is about 86% and 66% for PtSn/carbon (**Table 2**) and PtSn/Al_2O_3[37], respectively, and (ii) the Sn/Pt surface atomic ration is about 8 times higher for the carbon-supported samples[19]. Therefore, the amount of ionic tin is larger, and Pt particles are more blocked in the carbon-supported catalysts. These observations indicate higher alcohol selectivity, considering that ionic tin can activate the C=O bond, and blockage of the platinum particles reduces the rate of hydrogenation of the C=C bond.

According to the XAFS analysis, the bulk structure of platinum is similar in **PtSn/C–HP(CI)**, **PtSn/C–HP(SI)**, and **PtSn/Al_2O_3(CI)**, meaning that the effect of tin on Pt in these catalysts is similar. Considering that promotion by ionic tin does not occur in the hydrogenation of ketones[4], the effect of the platinum blockage is apparently the most important to modify the selectivity to alcohols. This could also be related to the slightly lower carvone conversion and slightly higher selectivity found for **PtSn/C–HP(SI)**, in which the Sn/Pt surface ratio is a little higher.

In general terms, the preparation method, (SI) or (CI), has little effect on the structure and the catalytic activity of PtSn catalyst prepared with the oxidized carbon support **C–HP**. The **PtSn/Al_2O_3(CI)** and **PtSn/Al_2O_3(SI)** catalysts reported previously show similar behavior[37].

On the other hand, a very important effect of the nature of the support has been observed. The selectivity to alcohols shown by carbon-supported PtSn catalysts has not been reported previously. The carbon material can have an effect because of its electronic properties, but can also cause a particular structure to be developed by the active phase after the reduction treatment.

4. Conclusions

The techniques used to characterize the PtSn/carbon catalysts indicate that:
(1) H_2PtCl_6 is partially reduced after the impregnation and drying steps. Successive impregnation and co-impregnation procedures have different effects on the reduction of Pt species in contact with the carbon surface and in the formation of surface oxygen complexes. Pt species interact more with the oxidized support.
(2) After impregnation and drying, Pt and Sn must be in close proximity.
(3) After reduction, bimetallic catalysts consist of metallic Pt, a major fraction of tin as Sn(Ⅱ) and/or Sn(Ⅳ) species (about 85%), and also Sn in the zero valent state (～15%), that is probably present as alloys with zero valent Pt. Sn surface enrichment has been observed. The presence of bimetallic PtSn phases, Pt particles, and Pt–O–Sn^{2+} species is also suggested by the XAFS results. Catalysts prepared with the oxidized support show a similar structure, regardless of the preparation method, whereas catalysts prepared with the original carbon support develop quite different structures.

The measurements of catalytic activity indicate that:
(1) The effect of the surface oxidation on the catalytic activity for cyclohexane dehydrogenation is related to the accessibility of the platinum particles, which are more externally located on the oxidized support.

(2) The effect of tin on the selectivity for alcohols is related to blockage of the platinum particles, which reduces the hydrogenation rate of the C=C bond. The carbon material affects the selectivity because of the influence on the structure developed by the active phase and because of the effect on the electronic properties of platinum, weakening the substrate adsorption and, thus, hindering the hydrogenation to saturated products.

Acknowledgments

The authors thank the Spanish CICYT and DGICYT (projects AMB96-0799 and QUI97-2051-CE), the Secretary for Science and Technology of the UNL (Argentina), programs CAI+D, and the Photon Factory (Japan), project 2001 G119, for financial support.

References

1) Sinfelt, J. H., "Bimetallic Catalysts: Discoveries, Concepts and Applications," Wiley, New York (1983).
2) Ponec, V., Bond, G. C. (eds.), "Catalysis by Metals and Alloys (Stud. Surf. Sci. Catal., vol. 95)," Elsevier Science, (1995), p. 583.
3) Paál, Z., "Catalytic Naphtha Reforming," eds. by Antos, G. J., Artami, A. M., Parera, J. M., Decker, New York (1995), p. 19.
4) Ponec, V., *Appl. Catal. A: General*, **149**, 27 (1997).
5) Srinivasan, R., Davis, B. H., *J. Mol. Catal*., **88**, 343 (1994).
6) Lei, Y. J., *Appl. Catal*., **72**, 33 (1991).
7) Kappenstein, C., Saouabe, M., Guérin, M., Marecot, P., Uszkurat, I., Paál, Z., *Catal. Lett*., **31**, 9 (1995).
8) Llorca, J., Homs, N., Fierro, J. L. G., Sales, J., Ramírez de la Piscina, P., *J. Catal*., **166**, 44 (1997).
9) Passos, F. B., Aranda, D. A. G., Schmal, M., *J. Catal*., **178**, 478 (1998).
10) de Miguel, S. R., Román-Martínez, M. C., Jablonski, E. L., Fierro, J. L. G., Cazorla-Amorós, D., Scelza, O. A., *J. Catal*., **184**, 514 (1999).
11) Román-Martínez, M. C., Cazorla-Amorós, D., Yamashita, H., de Miguel, S. R., Scelza, O. A., *Langmuir*, **16**, 1123 (2000).
12) Coloma, F., Sepúlveda-Escribano, A., García Fierro, J. L., Rodriguez-Reinoso, F., *Appl. Catal. A: General*, **136**, 231 (1996).
13) Larese, C., Campos-Martín, J. M., Calvino, J. J., Blanco, G., Fierro, J. L. G., Kang, Z. C., *J. Catal*., **208**, 467 (2002).
14) Huidobro-Pahissa, A., PhD. Thesis, University of Alicante, Spain, 2003.
15) de Miguel, S. R., Castro, A. A., Scelza, O. A., García Fierro, J. L., Soria, J., *Catal. Lett*., **36**, 201 (1996).
16) Ramallo-López, J. M., Santori, G. F., Giovanetti, L., Casella, M. L., Ferreti, O. A., Requejo, F. G., *J. Phys. Chem. B*, **107**, 11441 (2003).
17) Li, Y. X., Klabunde, K. J., Davis, B. H., *J. Catal*., **128**, 1 (1991).
18) Margitfalvi, J. L., Vankó, Gy., Borbáth, I., Tompos, A., Vértes, A., *J. Catal*., **190**, 474 (2000).
19) de Miguel, S. R., Román-Martínez, M. C., Cazorla-Amorós, D., Jablonski, E. L., Scelza, O. A., *Catal. Today*, **66**, 289 (2001).
20) Caballero, A., Dexpert, H., Didillon, B., LePletier, F., Clause, O., Lynch, J., *J. Phys. Chem*., **97**, 11283 (1993).
21) Borgna, A., Stagg, S. M., Resasco, D. E., *J. Phys. Chem*., **102**, 5077 (1998).
22) Lytle, F. W., Greegor, R. B., Marques, E. C., Biebesheimer, V. E., Sandstrom, D. R., Horseley, J. A., Via, G. H., Sinfelt, J. H., "Catalysts Characterization Science, Surface and Solid State Chemistry," eds. by Deviney, M. L., Gland, J. L., American Chemical Society, Washington DC (1985), p. 280.
23) Koningsberger, D. C., Prins, R. (eds.), "X-ray Absorption: Principles and Applications, Techniques of EXAFS, SEXAFS and XANES," John Wiley, New York (1988).
24) Conesa, J. C., Esteban, P., Dexpert, H., Bazin, D., "Spectroscopic Characterization of Heterogeneous Catalysts, A: Methods of Surface Analysis (Stud. Surf. Sci. Catal., vol. 57)," ed. by Fierro, J. L. G., Elsevier, (1990), p. A225.
25) Iwasawa, Y. (ed.), "X-ray Absorption Fine Structure for Catalysts and Surfaces. Series on Synchrotron Radiation. Techniques and Applications," vol. 2, World Scientific, Singapore (1996).
26) Cárdenas, G., Oliva, R., Reyes, P., Rivas, B. L., *J. Mol. Catal. A*, **191**, 75 (2003).
27) Hammoudeh, A., Mahmoud, S., *J. Mol. Catal. A*, **203**, 231 (2003).
28) Radovic, L. R., Rodríguez-Reinoso, F., "Chemistry and Physics of Carbon," vol. 25, (1997), p. 243.
29) Auer, E., Freund, A., Pietsch, J., Tacke, T., *Appl. Catal. A: General*, **173**, 259 (1998).
30) Román-Martínez, M. C., Cazorla-Amorós, D., Salinas-Martínez de Lecea, C., Linares-Solano, A., *Curr. Top. Catal*., **1**, 17 (1997).
31) Román-Martínez, M. C., Cazorla-Amorós, D., Linares-Solano, A., Salinas-Martínez de Lecea, C., *Carbon*, **31**, 895 (1993).
32) de Miguel, S. R., Scelza, O. A., Román-Martínez, M. C., Salinas-Martínez de Lecea, C., Cazorla-Amorós, D., Linares-Solano, A*., Appl. Catal. A: General*, **170**, 93 (1998).
33) Román-Martínez, M. C., Cazorla-Amorós, D., Linares-Solano, A., Salinas-Martínez de Lecea, C., Yamashita, H., Anpo, M., *Carbon*, **33**, 3 (1995).
34a) Román-Martínez, M. C., Cazorla-Amorós, D., Linares-Solano, A., Salinas-Martínez de Lecea, C., *Appl. Catal. A: General*, **116**, 187 (1994).
34b) Román-Martínez, M. C., Cazorla-Amorós, D., Linares-Solano, A., Salinas-Martínez de Lecea, C., *Appl. Catal. A: General*, **134**, 159 (1994).
35) Román-Martínez, M. C., Cazorla-Amorós, D., Linares-Solano, A., Salinas-Martínez de Lecea, C., *Langmuir*, **12**, 379 (1996).
36) Baronetti, G. T., de Miguel, S. R., Scelza, O. A., Castro, A. A., *Appl. Catal*., **24**, 109 (1986).
37) Jablonski, E. L., Ledesma, S., Torres, G. C., de Miguel, S. R., Scelza, O. A., *Catal. Today*, **48**, 65 (1999).
38) Torres, G. C., Jablonski, E. L., Baronetti, G. T., Castro, A. A., de Miguel, S. R., Scelza, O. A., Blanco, M. D., Peña, M. A., Fierro, J. L. G., *Appl. Catal*., **161**, 213 (1997).
39) van Dam, H. E., van Bekkum, H., *J. Catal*., **131**, 335 (1991).
40) Czaran, E., Finster, J., Schnabel, K.-H., *Z. Anorg. Allg. Chem*., **443**, 175 (1978).
41) Coloma, F., Sepúlveda, A., Fierro, J. L. G., Rodríguez-Reinoso, F., *Langmuir*, **10**, 750 (1994).
42) Vilella, I. M. J., PhD. Thesis, Universidad Nacional del Litoral, Santa Fe, Argentina, 2003.
43) Spieker, W. A., Liu, J., Miller, J. T., Kropf, A. J., Regalbuto, J. R., *Appl. Catal. A: General,* **232**, 219 (2002).
44) Calo, J. M., Cazorla-Amorós, D., Linares-Solano, A., Román-Martínez, M. C., Salinas-Martínez de Lecea, C., *Carbon*, **35**, 543 (1997).
45) "Handbook of X-ray Photoelectron Spectroscopy," Perkin Elmer Corp., (1979); Briggs, D., Seah, M. P., "Practical Surface Analysis," Wiley, New York (1983).
46) Lau, C. L., Wertheim, G. K., *J. Vac. Sci. Technol*., **15**, 622 (1978).
47) Meitzner, G., Via, G. H., Lytle, F. W., Sinfelt, J. H., *J. Phys. Chem*., **96**, 4960 (1992).

48) Stern, E. A., Kim, K., *Phys. Rev. B*, **23**, 3781 (1981).
49) Pinxt, H. H. C. M., Kuster, B. F. M., Koningsberger, D. C., Marin, G. B., *Catal. Today*, **39**, 351 (1998).
50) Bailar, J. C., Emeléus, H. J., Nyholm, R., Trotman-Dickenson, A. F., "Comprehensive Inorganic Chemistry," vol. 2, Pergamon, Oxford (1973), p. 53.
51) Meitzner, G., Via, G. H., Lytle, F. W., Fung, S. C., Sinfelt, J. H., *J. Phys. Chem*., **92**, 2925 (1988).
52) Stagg, S. M., Romeo, E., Padro, C., Resasco, D. E., *J. Catal*., **178**, 137 (1998).
53) Gómez, R., Arredondo, J., Rosas, N., del Angel, G., "Heterogeneous Catalysis and Fine Chemicals Ⅱ," eds. by Guisnet, M. *et al.*, Elsevier Science Publishers B. V., Amsterdam (1991), p. 185.
54) del Angel, G., Melendrez, R., Bertin, V., Domínguez, J. M., Marecot, P., Barbier, J., "Heterogeneous Catalysis and Fine Chemicals Ⅲ," eds. by Guisnet, M. *et al.*, Elsevier Science Publishers B. V., Amsterdam (1993), p. 171.
55) Melendrez, R., del Angel, G., Bertin, V., Valenzuela, M. A., Barbier, J., *J. Mol. Catal. A*, **157**, 143 (2000).

要　　旨

カーボン担持 PtSn 触媒: キャラクタリゼーションと触媒特性

Maria Carmen Román-Martínez[†1)], Dego Cazorla-Amorós[†1)], Sergio de Miguel[†2)], Osvaldo Scelza[†2)]

[†1)] Departamento de Química Inorgánica, Facultad de Ciencias, Universidad de Alicante, Apartado 99, 03080 Alicante, SPAIN

[†2)] Instituto de Investigaciones en Catálisis y Petroquímica (INCAPE), Facultad de Ingeniería Química, Universidad Nacional del Litoral, CONICET, Santiago del Estero 2654 (3000) Santa Fe, ARGENTINA

市販の活性炭および 20 v/v% 過酸化水素水で酸化処理した活性炭を担体に用い，白金とスズを逐次的にまたは同時に担持することにより，カーボン担持 PtSn 触媒を調製した。触媒のキャラクタリゼーションを TPD，TPR，水素吸着，XPS，XAFS を用いて行った。また，触媒活性を評価するために，構造非敏感反応であるシクロヘキサンの脱水素，構造敏感反応であるシクロペンタンの水素化分解，およびカルボンの水素化を行った。カルボンの水素化では，カルボン分子内に水素化が可能な一つの C=O と二つの C=C 結合を有することから，触媒による選択性への影響を調べた。本研究の目的は，触媒の調製法や担体の性質と，触媒の特徴や触媒活性との関係を見い出すことである。担体の酸化処理により，カーボン担体の多孔度は変化し，反応物が活性点へ到達し易くなった。カルボンの水素化では，スズを加えることにより不飽和アルコールへの選択性が増加した。このことは，スズが白金粒子を覆うためであると推定した。また，担体の電子的特性により，あるいは担体が担持金属の特異な構造を形成することにより，カーボン担体自身も選択性に影響を及ぼすと考えた。